BJP BRITISH JOURNAL OF PHARMACOLOGY

BPS BRITISH PHARMACOLOGICAL SOCIETY

British Journal of Pharmacology (2009), 158, 361–371

0007-1188/09
www.brjpharmacol.org

THEMED ISSUE: GPCR

RESEARCH PAPER

Novel antagonists for proteinase-activated receptor 2: inhibition of cellular and vascular responses *in vitro* and *in vivo*

T Kanke[1]*, M Kabeya[1], S Kubo[2], S Kondo[1], K Yasuoka[1], J Tagashira[1], H Ishiwata[1], M Saka[1], T Furuyama[1], T Nishiyama[1], T Doi[1], Y Hattori[1], A Kawabata[2], MR Cunningham[3] and R Plevin[3]

[1]*Tokyo New Drug Research Laboratories, Kowa Company Limited, Noguchicho, Higashimurayama, Tokyo, Japan,* [2]*Division of Physiology and Pathophysiology, School of Pharmaceutical Sciences, Kinki University, Kowakae, Higashi-Osaka, Japan, and* [3]*Department of Physiology and Pharmacology, Strathclyde Institute for Biomedical Sciences, University of Strathclyde, Glasgow, Scotland, UK*

Background and purpose: Proteinase-activated receptor 2 (PAR_2) is a G-protein coupled receptor associated with many pathophysiological functions. To date, the development of PAR_2 antagonists has been limited. Here, we identify a number of novel peptide-mimetic PAR_2 antagonists and demonstrate inhibitory effects on PAR_2-mediated intracellular signalling pathways and vascular responses.

Experimental approach: The peptide-mimetic compound library based on the structures of PAR_2 agonist peptides were screened for inhibition of PAR_2-induced calcium mobilisation in human keratinocytes. Representative compounds were further evaluated by radioligand binding and inhibition of NFκB transcriptional activity and IL-8 production. The vascular effects of the antagonists were assessed using *in vitro* and *in vivo* models.

Key results: Two compounds, K-12940 and K-14585, significantly reduced SLIGKV-induced Ca^{2+} mobilisation in primary human keratinocytes. Both K-12940 and K-14585 exhibited competitive inhibition for the binding of a high-affinity radiolabelled PAR_2-ligand, [^{3}H]-2-furoyl-LIGRL-NH_2, to human PAR_2 with K_i values of 1.94 and 0.627 μM respectively. NFκB reporter activity and IL-8 production were also significantly reduced. Furthermore, relaxation of rat-isolated aorta induced by SLIGRL-NH_2 was inhibited competitively by K-14585. K-14585 also significantly lowered plasma extravasation in the dorsal skin of guinea pigs and reduced salivation in mice.

Conclusions and implications: K-12940 and K-14585 antagonized PAR_2 competitively, resulting in inhibition of PAR_2-mediated signalling and physiological responses both *in vitro* and *in vivo*. These peptide-mimetic PAR_2 antagonists could be useful in evaluating PAR_2-mediated biological events and might lead to a new generation of therapeutically useful antagonists.
British Journal of Pharmacology (2009) **158,** 361–371; doi:10.1111/j.1476-5381.2009.00342.x

This article is part of a themed issue on GPCR. To view this issue visit
http://www3.interscience.wiley.com/journal/121548564/issueyear?year=2009

Keywords: Proteinase-activated receptor 2 (PAR_2); antagonist; Ca^{2+} mobilization; keratinocytes; radioligand-binding

Abbreviations: 2-furoyl-LIGRL-NH_2, 2-furoyl-Leu-Ile-Gly-Arg-Leu-amide; HUVEC, human umbilical vein endothelial cells; PAR, proteinase-activated receptor; PMA, phorbol myristate acetate; SAR, structure-activity relationship; SLIGKV-OH, Ser-Leu-Ile-Gly-Lys-Val; SLIGRL-NH_2, Ser-Leu-Ile-Gly-Arg-Leu-amide; TNFα, tumour necrosis factorα

Introduction

Proteinase-activated receptor 2 (PAR_2), a member of the family of G-protein-coupled receptors [nomenclature follows Alexander *et al.* (2008)], is activated by proteases such as trypsin, tryptase and coagulation factors VIIa and Xa (Nystedt *et al.*, 1994; Molino *et al.*, 1997; Camerer *et al.*, 2000) cleaving the receptor to reveal an N-terminal 'tethered ligand', SLIGKV

Correspondence: Professor R Plevin, Department of Physiology and Pharmacology, Strathclyde Institute for Biomedical Sciences, University of Strathclyde, 27 Taylor Street, Glasgow, Scotland G4 0NR, UK. E-mail: r.plevin@strath.ac.uk
*Present address: Department of Pharmacology, Okayama University Graduate School of Medicine, Dentistry and Pharmaceutical Sciences, Okayama 700-8558, Japan.
Received 10 March 2009; accepted 24 March 2009

and SLIGRL for human and mouse/rat PAR_2, respectively, which subsequently interacts with the activation domain of the receptor, initiating intracellular signalling pathways and functional responses (Macfarlane *et al.*, 2001; Hollenberg, 2005; Steinhoff *et al.*, 2005).

A number of studies have demonstrated a wide range of important physiological roles for PAR_2. Although PAR_2 plays protective roles in several biological systems, such as the lung (Cocks and Moffatt, 2000; Lan *et al.*, 2000; 2001) and gastrointestinal tract (Kawabata *et al.*, 2001; Kawao *et al.*, 2002), there is much evidence that activation of PAR_2 is pro-inflammatory. For instance, the PAR_2 activating peptide elicits inflammatory responses in the rat hind paw (Kawabata *et al.*, 1998; Vergnolle *et al.*, 1998), mouse knee joint (Ferrell *et al.*, 2003) and mouse colon (Cenac *et al.*, 2002). A critical role of PAR_2 has also been demonstrated in skin (Kawagoe *et al.*, 2002) and neurogenic inflammation (Ricciardolo *et al.*, 2000; Steinhoff *et al.*, 2000). Therefore, antagonists for PAR_2 would be appropriate for the treatment of these inflammatory conditions. Currently, however, there is only limited published information available for the development of PAR_2 antagonists.

Recently, several approaches have been demonstrated to inhibit PAR_2-mediated responses utilizing pepducins (Kaneider *et al.*, 2007), siRNA and monoclonal antibodies (Kelso *et al.*, 2006). A low molecular weight compound which mimics the peptide structure of truncated PAR_2 agonist peptide inhibited PAR_2-induced joint inflammation *in vivo* (Kelso *et al.*, 2006), although its molecular mechanisms of receptor blockade were not clear. So far, there are no reports of competitive antagonists for this receptor.

We have previously identified a series of modified PAR_2 agonist peptides, substituted with 2-furoyl on the N-terminal serine residue of native PAR_2-activating peptides, which were shown to be potent and metabolically stable both *in vivo* and *in vitro* (Ferrell *et al.*, 2003; Kawabata *et al.*, 2004). Utilizing the radiolabelled potent PAR_2-activating peptide, [^{3}H]2-furoyl-LIGRL-NH_2, we have established a PAR_2 receptor binding system, which enabled us to characterize binding profile of agonists/antagonists to human PAR_2 (Kanke *et al.*, 2005). By analysing the structure-activity relationship (SAR) of PAR_2 agonists, we found the affinity of the ligand and the receptor activation potency were regulated relatively independently by several critical sites of the peptide structures. Therefore, we thought it could be possible to identify PAR_2 antagonists, possessing high affinity to the receptor binding site but not activating the receptor, through screening of peptide-mimetic compound libraries. As a result of extensive screening, we have identified a series of peptide-mimetic compounds that inhibit Ca^{2+} responses in human keratinocytes. Two representative compounds, K-12940 and K-14585 (Figure 1), were competitive inhibitors of the binding of [^{3}H]-2-furoyl-LIGRL-NH_2, to human PAR_2. Both compounds were also found to be able to inhibit a variety of previously characterized intracellular responses including activation of NFκB and the production of IL-8. Furthermore, the inhibitory effects of K-14585 on PAR_2-mediated *in vitro* and *in vivo* tissue responses were demonstrated including relaxation of the rat aorta, increased vascular permeability and saliva production. These results have identified novel peptide mimetic antagonists for PAR_2 which could be therapeutically useful for the treatment of PAR_2-related inflammatory diseases.

Methods

Cell culture

Normal human epidermal keratinocytes (NHEK) which strongly expressed PAR_2 (Santulli *et al.*, 1995; Scott *et al.*, 2004) were obtained from Cambrex (Walkersville, MD, USA) and cultured in the complete keratinocyte growth medium. The human skin epithelial cell line NCTC2544 expressing human PAR_2, designated as NCTC2544-PAR_2 cells, was described previously (Kanke *et al.*, 2001). Control NCTC2544 cells (WT-NCTC2544 cells) were grown in Medium 199 with Earle's salts (Sigma-Aldrich, MO, USA) containing 10% ($v \cdot v^{-1}$) fetal calf serum (FCS), sodium bicarbonate (50 mM), L-glutamine (2 mM), penicillin (100 $U \cdot mL^{-1}$) and streptomycin (100 $\mu g \cdot mL^{-1}$). NCTC2544-PAR_2 cells were cultured in complete medium containing geneticin (400 $\mu g \cdot mL^{-1}$) to maintain selection pressure. Human embryonic kidney 293 cells (HEK293 cells) were maintained in 10% minimal essential medium (MEM with Earle's salts, L-glutamine supplemented with 10% ($v \cdot v^{-1}$) FCS, 1% penicillin, 1% streptomycin, 1% non-essential amino acids). All cells were grown at 37°C in an incubator with saturated humidity and 5% CO_2 and NCTC2544 cells were passaged using Versene [0.53 mM ethylenediaminetetraacetic acid (EDTA) in phosphate buffered saline (PBS)] to avoid trypsin exposure. NHEK were passaged with trypsin, and passages at 4–8 were used for the experiments. HEK293 cells were passaged using 1xSSC (sodium citrate, pH 7.4).

Transient transfection of PAR_1, PAR_2 and PAR_4 in HEK293 cells

HEK293 cells were grown to 70–80% confluence on 12 well plates and transiently transfected with 1 μg/well Wild type PAR_1, PAR_2 or PAR_4 plasmid DNA using the Lipofectamine™ 2000 transfection system according to manufacturer's guidelines. After a 4 h incubation period with the DNA mixture in OptiMEM (Invitrogen Ltd, Paisley, UK) with no serum or antibiotics, the OptiMEM was replaced with complete medium for another 20 h. Measurement of [^{3}H]inositol phosphate accumulation stimulated by PAR-specific activating peptide was measured in these cells pre-labelled overnight with [^{3}H]2-myoinositol in serum free medium as outlined previously (Plevin *et al.*, 1994). During this time, cells were rendered quiescent by serum deprivation. Test compounds were added 30 min prior to agonist stimulation with various PAR-specific activating peptides for 1 h.

Measurement of Ca^{2+} mobilization

PAR_2-mediated intracellular calcium mobilization in normal human keratinocytes was measured with minor modifications of a previously described method (Kawabata *et al.*, 2004) using a 96-well scanning fluorimeter, FlexStation (Molecular Devices, Wokingham, UK). Human normal keratinocytes (30 000 cells per well) were seeded in black-wall clear-bottom 96-well plates (Corning B.V. Life Sciences, Koolhovenlaan, the

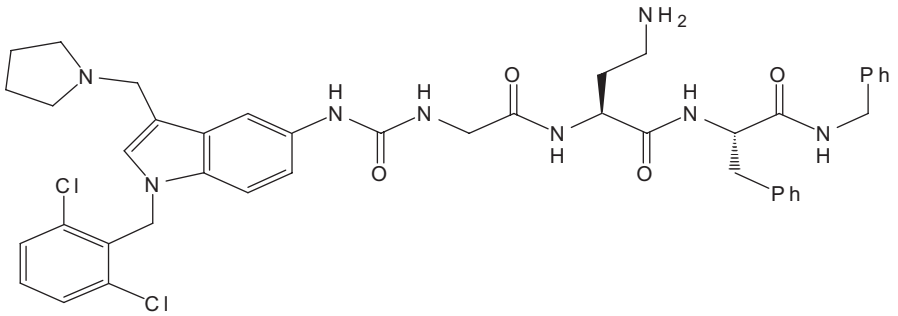

K-12940

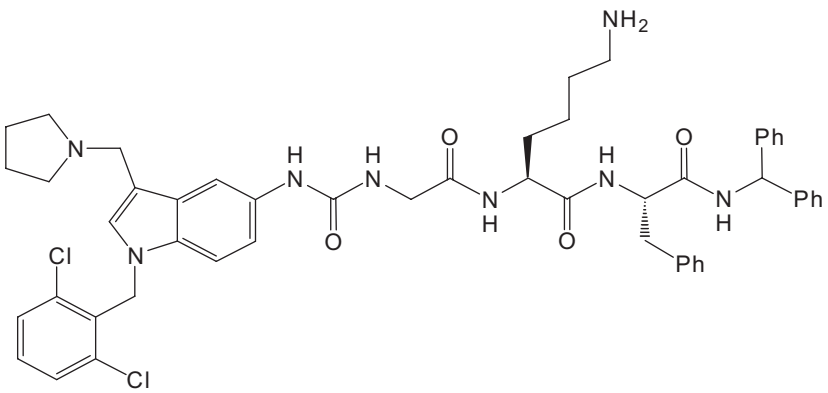

K-14585

Figure 1 Chemical structures of peptide-mimetic proteinase-activated receptor 2 antagonists K-12940 and K-14585.

Netherlands) 24 h prior to the assay and grown to reach confluence. Cells were washed once with keratinocyte basic medium (KBM) and replaced with 80 mL of KBM. Subsequently, 80 μL of calcium assay dye solution (FLEXstation Calcium 3 Assay kit, Molecular Devices) dissolved in Hank's balanced salt solution (HBSS)(pH 7.4) containing 2.5 mM probenecid was added and incubated for 60 min at 37°C. Test compounds were added 30 min prior to the agonist stimulation. Then cells were stimulated with various concentrations of agonists prepared in HBSS and the fluorescence change measured at 25°C (excitation 485 nm and emission 525 nm). Antagonists were added 30 min prior to the agonist stimulation. Inhibitory effects of antagonists on calcium responses (max–min) were expressed as percentage of the reference calcium response induced by either PAR_2 agonist peptide SLIGKV-OH (30 μM) or histamine (30 μM) alone. The half-maximal effective concentration values (IC_{50}) were estimated from the concentration-response curve.

NFκB-luciferase reporter gene assay

PAR_2 agonist-activated transcriptional activation of NFκB was determined utilizing NFκB-luciferase reporter gene system as described previously (Macfarlane *et al.*, 2005) The plasmid vector containing repeated consensus sequence of NFκB binding cis-elements, ×4 NFκB, connected to the firefly luciferase gene was stably transfected into the NCTC2544-PAR_2 cells and a positive clone was used for the assay. In the assay, the cells were detached from flasks using Versene and seeded into white 96-well plates (96F Nunclon Delta, Thermo Scientific Nunc, Leicestershire, UK) with 30 000 cells per well. Cells were grown until sub-confluent (18–24 h) at 37°C. Then, cells were washed with serum free medium once and rendered quiescent with serum free medium for 18 h. Test compounds dissolved in dimethyl sulfoxide (DMSO) were diluted in serum free medium at appropriate concentrations and was added to the cells to preincubate for 15–30 min. Subsequently, cells are stimulated with agonists such as SLIGKV, trypsin or phorbol myristate acetate (PMA) for 6 h at 37°C. Stimulation was terminated by adding 100 μL per well of luciferase assay reagent (Bright-Glo, Promega UK Ltd., Hampshire, UK) and luminescence was measured with 96-well luminometer (MicroLUMAT LB96P, EG&G Berthold UK, Herts, UK).

ELISA for interleukin (IL)-8

NCTC2544-PAR_2 cells seeded in 24-well plates were stimulated with PBS (Control), SLIGKV (100 μM) or tumour necrosis factorα (TNFα;10 ng·mL^{-1}) in the absence or presence of

antagonists (5 μg·mL^{-1}) for 24 h. IL-8 levels in the culture medium were determined by enzyme-linked immunosorbent assay (ELISA) according to the manufacturer's instructions TECHNE (Bibby-Scientific Ltd, Staffordshire, UK). Data are expressed as the mean and SEM of three experiments.

PAR_2 ligand-binding assay

PAR_2 ligand-binding assay was performed using [^{3}H]2-furoyl-LIGRL-NH_2 as described previously (Kanke *et al.*, 2005). NCTC2544-PAR_2 cell suspension (0.2 mL, 3.0×10^5 cells) were incubated at 25°C along with [^{3}H]2-furoyl-LIGRL-NH_2 (9.2 nM, 1 μCi·mL^{-1}) in either absence or presence of agonists and antagonists. The cell-bound radioligand was separated by centrifugation and the radioactivity was measured by scintillation counting (Tri-Carb 2700TR, PerkinElmer, MA, USA). The amount of specific binding was calculated by subtraction from the total amount of the radioligand bound in the absence of competing ligands, non-specific binding in the presence of an excess (100 μM) of unlabeled 2-furoyl-LIGRL-NH_2. Competition studies with various PAR_2 agonists and antagonists were performed and the displacement curve for each agonist/antagonist was constructed by measuring the percentage of the specific [^{3}H]2-furoyl-LIGRL-NH_2 binding (% specific binding) in the presence of each peptide concentration, relative to the maximum specific binding in the absence of unlabelled 2-furoyl-LIGRL-NH_2.

Experimental animals

All animal care and experimental procedures conformed to the Guide for the Care and Use of Laboratory Animals published by the US National Institutes of Health.

Relaxation of rat-isolated thoracic aorta

Male Wistar rats (8–9 weeks, 300–350 g; Japan SLC. Inc., Kotocho, Nishi-Ku, Japan) were killed by decapitation under urethane (1.5 g·kg^{-1}, i.p.) anaesthesia, and the thoracic aorta was removed. Endothelium-intact, rings of thoracic aorta (4 mm long) were placed in 2 mL organ bath filled with gassed Krebs Hensleit solution (composition in mM: NaCl, 118; KCl, 4.7; $CaCl_2$, 2.5; $MgCl_2$, 1.2; $NaHCO_3$, 25; KH_2PO_4, 1.2; glucose, 10) maintained at 37°C and bubbled with 95% O_2, 5% CO_2. The segment was allowed to equilibrate for 1 h under a resting tension of 10 mN, and isometric tension was recorded through a force-displacement transducer (UL-10GR, Minebea Co., Ltd., Meguro-Ku, Tokyo, Japan). SLIGRL-NH_2 (1-100 μM) was cumulatively applied in the absence or presence of K-14585 (10 μM) to aortic rings precontracted with phenylephrine (1 μM) and relaxation of the rings was measured. Data are expressed as percent of relaxation calculated as percent of the maximum relaxation induced by papaverine (100 μM).

Cutaneous microvascular permeability in guinea pigs

Male Hartley guinea pigs (450–550 g, Japan SLC. Inc., Japan) were used for the experiments. Under urethane (1.5 g·kg^{-1}, i.p.) anaesthesia, Evans blue dye (50 mg·kg^{-1}) was injected intravenously, and immediately after, either vehicle (10% DMSO), SLIGRL-NH_2 (300 nM) or a mixture of SLIGRL-NH_2 (300 nM) and K-14585 (300 μg) was injected intradermally. We used eight sites per guinea pig, approximately 20 mm apart, on dorsal skin shaved a day before the experiments. Intradermal injections were made in a volume of 100 μL per site. Thirty minutes after the intradermal injections, the animal was killed and the increase of vascular permeability was assessed by measuring the amount of extravasated dye in the injection sites. Dorsal skin was removed from the animal and the sites of injection (approximately 15 mm in diameter) were punched out and dissolved in 1.4 mL of 1N KOH at 37°C overnight. The dye was extracted with 18.6 mL of a mixture of 0.6N H_3PO_4 and acetone (5:13, v: v^{-1}) per site and quantified using a spectrophotometer at 620 nm with standard curve of Evans blue in the same solvent at concentrations of 0.1–30 μg·mL^{-1}.

Secretion of saliva in anaesthetized mice in vivo

Salivary exocrine secretion was assessed in male ddY mice (8–10 weeks old; 20–25 g) under urethane anaesthesia (i.p., 1.5 g·kg^{-1}), as described elsewhere (Takeda and Krause, 1989; Kawabata *et al.*, 2000). Small pre-weighed pads of cottonwool were placed in the mouth and replaced with new pads every 5 min. The difference in weight of the pads before and after being placed in the mouth was taken to represent the amount of saliva secreted in each period. Salivation was monitored for 15 min after i.p. challenge with agonists. Amastatin (Peptide Institute, Minoh, Japan), an inhibitor of aminopeptidase, a degradation enzyme for peptides, was administered i.p. immediately before agonists. Antagonists were given i.p. 5 min before the agonist challenge.

Data analysis

For calcium mobilization studies, the peak fluorescence change was plotted versus the concentration of agonists and the concentration-response curve fitted using a four-parameter logistic equation to determine the EC_{50} value. Radioligand binding data were analysed by nonlinear regression analysis using GraphPad Prism 4 (GraphPad Software, CA, USA). The displacement curves by agonists/antagonists were assumed to fit to a one-site model to determine IC_{50} values. The inhibitor constant, K_i of each agonist/antagonist was then derived from the IC_{50} and the K_d of 2-furoyl-LIGRL-NH_2.

Data are represented as mean ± SEM. Statistical significance was analyzed by Student's *t*-test for two group data. Significance was set at a $P < 0.05$ level.

Materials

Preparation of PAR_2 antagonists. Peptide mimetic PAR_2 antagonists (Figure 1), K-12940, {(N-[1-(2,6-dichlorophenyl)methyl]-3-(1-pyrrolidinylmethyl)-1H-indol-5-yl)aminocarbonyl}-glycinyl-L-α,γ-diaminobutyryl-L-phenylalaninyl-N-benzylamide and K-14585 {(N-[1-(2,6-dichlorophenyl)methyl]-3-(1-pyrrolidinylmethyl)-1H-indol-5-yl)aminocarbonyl}-glycinyl-L-lysinyl-L-phenylalanyle-N-benzhydrylamide were synthe-

sized at Kowa Tokyo New Drug Research Laboratories (Tokyo, Japan). The chemical structures were confirmed by nuclear magnetic resonance and mass spectrometry (MS). The purity of compounds (>95%) was determined by high-performance liquid chromatography (HPLC). The compounds were dissolved in DMSO and aliquots were kept at –20°C until use.

PAR_2-activating peptide and other chemicals. The human PAR_2-activating peptide, Ser-Leu-Ile-Gly-Lys-Val (SLIGKV-OH), mouse/rat PAR_2-activating peptide, SLIGRL-NH_2, Ser-Leu-Ile-Gly-Arg-Leu-amide; and a highly potent PAR_2-activating peptide, 2-furoyl-Leu-Ile-Gly-Arg-Leu-amide (2-furoyl-LIGRL-NH_2) (Kawabata *et al.*, 2004) were synthesized and purified (>95%) by HPLC, and the structures were confirmed by MS. The radiolabelled PAR_2-activating peptide, [^{3}H]2-furoyl-LIGRL-NH_2 (radiochemical purity of 99.4%, specific activity of 4.03 TBq·mM), was prepared for us by Amersham Biosciences (Buckinghamshire, UK) as described previously (Kanke *et al.*, 2005). Trypsin from bovine pancreas (9300 unit·mg^{-1}), A23187 and probenecid were obtained from Sigma-Aldrich Co. Histamine dihydrochloride, dibutyl phthalate and dinonyl phthalate were purchased from Wako Pure Chemical Industries (Osaka, Japan).

Results

Inhibitory effects of peptide antagonists on PAR_2 agonist peptide-induced Ca^{2+} mobilization in human keratinocytes

Initially, a series of potential PAR_2 antagonist compounds including K-14584 and K-12940 (Figure 1) were screened for their ability to inhibit PAR_2 mediated Ca^{2+} mobilization in primary cultures of human keratinocytes, a cell type known to express PAR_2 (Santulli *et al.*, 1995). SLIGKV-OH stimulated a rapid increase in intracellular Ca^{2+} which peaked within 60 s of stimulation (Figure 2). Pre-incubation with K-14585 (Figure 2) resulted in a significant decrease in this induced Ca^{2+} mobilization, of approximately 60% over a number of experiments (Table 1). Several additional compounds including K-12940 were screened and inhibition assessed (see Table 1). From these compounds, K-14585 and K-12940 were then assessed in a number of other assays and *in vitro* and *in vivo* systems to determine if the relative difference in effectiveness in the Ca^{2+} mobilization assays between the two compounds were reflected in other test systems.

To examine the direct effect of both K-12940 and K-14585 upon PAR_2 receptor binding, we utilized a radioligand binding assay previously established and characterized in the laboratory (Kanke *et al.*, 2005). Initially, using competition curves for the binding of [^{3}H]-2-furoyl-LIGRL-NH_2 to plasma membranes from NCTC2544-PAR_2 cells we established an order of potency for the agonist peptides to confirm the pharmacological identity of the binding site (Table 2). All PAR_2-activating peptides exhibited concentration-dependent displacement of specific [^{3}H]-2-furoyl-LIGRL-NH_2 binding to NCTC2544-PAR_2 cells. The order of the affinity of the displacing peptides was: 2-furoyl-LIGRL-NH_2 > 2-furoyl-LIGKV-NH_2 > 2-furoyl-LIGRL-OH > 2-furoyl-LIGKV-OH > SLIGRL-NH_2 > SLIGKV-NH_2 > SLIGRL-OH > SLIGKV-OH. The calculated Ki value from the displacement curve for each agonist and its relative binding affinity to the original peptide, SLIGKV-OH, are shown in Table 2 and compared with EC_{50} values for the Ca^{2+} assay in the same cells as described previously (Kawabata *et al.*, 2004). There was minimal binding competition for [^{3}H]-2-furoyl-LIGRL-NH_2 binding by the inactive reverse PAR_2 peptide LRGILS-NH_2 while the PAR_1 selective agonist peptide, TFLLRN-NH_2, reduced the [^{3}H]-2-furoyl-LIGRL-NH_2 binding only at high concentrations and its estimated Ki value was higher than 1 mM.

Using the radioligand binding assay, the characteristics of displacement by K-12940 and K-14585 were further analysed (Figure 3). Both compounds displaced [^{3}H]-2-furoyl-LIGRL-NH_2 binding in the low to mid-micromolar range, giving Ki values of 1.94 and 0.627 μM respectively (Table 3). Hill slopes of close to unity suggested one site binding although insufficient material was available to generate enough data points to assess this fully. Furthermore, the peptide-mimetic antagonists did not reduce non-specific [^{3}H]2-furoyl-LIGRL-NH_2

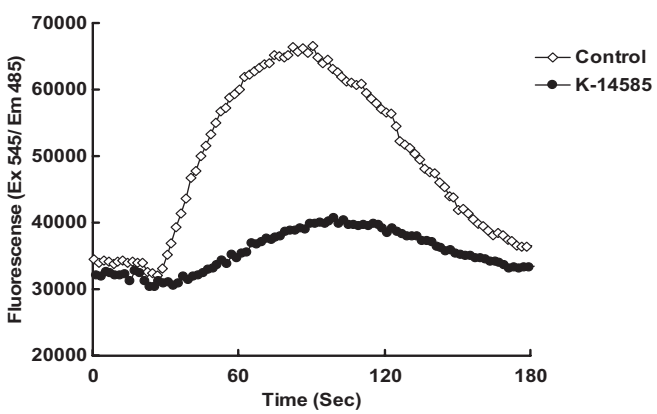

Figure 2 Representative trace for inhibitory effect of K-14585 on SLIGKV-induced Ca^{2+} mobilization in normal human epidermal keratinocytes. Cells were stimulated with SLIGKV (100 μM), and intracellular Ca^{2+} mobilization was measured using a fluorescence method as described in the Methods section. K-14585 (10 μM) was incubated with cells 15 min prior to addition of agonist peptide. Fluorescence was measured over 180 s.

Table 1 Inhibitory effects of PAR_2 antagonists on Ca^{2+} mobilization in human keratinocytes

Compound	*% Inhibition*	
	Mean	*SEM*
K-12940	33.6	16.8
K-13412	15.1	10.5
K-14324	14.2	10.0
K-14458	32.0	2.3
K-14585	58.4	13.0
K-14773	52.2	1.8

$n = 4$.
Human keratinocytes were pre-treated with 10 μM of test compound and stimulated with 30 μM PAR_2 agonist peptide, SLIGKV-OH. Intracellular Ca^{2+} was assessed as outlined in the Methods section.
Structures of K-14585 and K-12940 are shown in Figure 1; structures of the other compounds in the Table can be found in Mototsugu *et al.* (2007).
PAR_2, proteinase-activated receptor 2; SLIGKV-OH, Ser-Leu-Ile-Gly-Lys-Val.

Table 2 Comparison of PAR_2 agonist peptides on binding competition and potency on Ca^{2+} mobilization in NCTC2544PAR_2 cells

	Binding assay			*Ca^{2+} mobilization*		
	K_i (μM)		*Relative to SLIGKV-OH*	*EC_{50} (μ M)*		*Relative to SLIGKV-OH*
	Mean	*(SEM)*		*Mean*	*(SEM)*	
SLIGKV-OH	50.3	(4.77)	1	0.54	(0.078)	1
SLIGRL-OH	15.5	(4.76)	3.25	0.20	(0.070)	2.70
SLIGKV-NH_2	9.64	(1.21)	5.24	0.075	(0.0072)	7.20
SLIGRL-NH_2	2.61	(0.37)	19.3	0.046	(0.019)	11.7
2-furoyl-LIGKV-OH	2.57	(0.67)	19.6	0.067	(0.011)	8.06
2-furoyl-LIGRL-OH	0.65	(0.064)	77.9	0.024	(0.0069)	22.5
2-furoyl-LIGKV-NH_2	0.30	(0.053)	166	0.0076	(0.00076)	71.1
2-furoyl-LIGRL-NH_2	0.11	(0.011)	449	0.0050	(0.0017)	108
tc-LIGRLO- NH_2	14.0	(2.49)	3.59	n.d.	n.d.	n.d.
TFLLR- NH_2	1177	(952.2)	0.043	n.d.	n.d.	n.d.

Binding data was generated as outlined in the Methods section and compared with data on Ca^{2+} mobilization from (Kawabata *et al.*, 2004). Each value is obtained from at least four separate experiments.
n.d., not determined; PAR_2, proteinase-activated receptor 2; SLIGKV-OH, Ser-Leu-Ile-Gly-Lys-Val; SLIGRL-NH_2, Ser-Leu-Ile-Gly-Arg-Leu-amide; 2-furoyl-LIGRL-NH_2; 2-furoyl-Leu-Ile-Gly-Arg-Leu-amide.

Table 3 Comparative K_i values for displacement of [^{3}H]2-furoyl-LIGRL-NH_2 binding to PAR_2 and inhibition of luciferase expression

	Binding assay K_i (μM)			*Luciferase assay IC_{50} (μM)*	
	Mean	*(SEM)*	*Relative to SLIGKV-OH*	*Mean*	*(SEM)*
SLIGKV-OH	50.3	(4.77)	1	n.d	n.d
2-furoyl-LIGRL-NH_2	0.11	(0.011)	449	n.d	n.d
K-12940	1.94	(0.47)	27.9	2.87	0.48
K-14585	0.63	(0.14)	86.3	1.10	0.07

Binding data was generated as outlined in the Methods section. Each value is obtained from at least four separate experiments.
PAR_2, proteinase-activated receptor 2; SLIGKV-OH, Ser-Leu-Ile-Gly-Lys-Val; 2-furoyl-LIGRL-NH_2; 2-furoyl-Leu-Ile-Gly-Arg-Leu-amide.

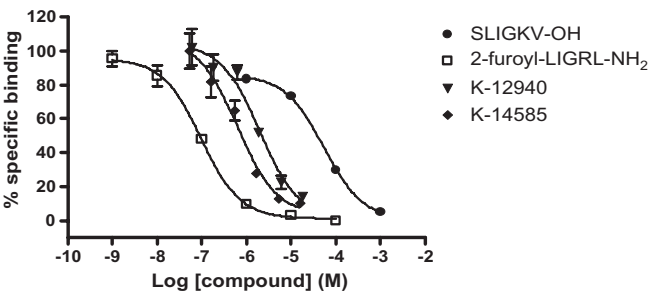

Figure 3 Displacement of [^{3}H]2-furoyl-LIGRL-NH_2 binding in NCTC2544-PAR_2 cells by K-12940 and K-14585. Cells were incubated with [^{3}H]2-furoyl-LIGRL-NH_2 (9.2 nM, 1 μCi·mL^{-1}) in either absence or presence of increasing concentrations of unlabelled agonist/antagonist under conditions as outlined in the Methods section. Binding competition curves for unlabelled compounds are presented as % specific binding. Results are shown as the mean ± SEM (n = 3).

binding to either PAR_2 expressing parental cells (data not shown) confirming specific inhibition of PAR_2 receptor binding.

We next sought to assess the antagonist effect of K-12940 and K-14585 on a number of cellular markers relevant to functional end points. Using PAR_2 expressing NCTC2544 cells, we initially measured [^{3}H]IP production and found significant inhibition of SLIGKV stimulation using the maximum concentration of antagonist (10 μM) (% inhibition, mean ± SEM; K-12940 = 36 ± 1.1% n = 4, K-14858 = 62 ± 3.2%, n = 4, P > 0.01, compared with SLIGKV alone). We used the same cell line additionally expressing the NFκB reporter luciferase gene, which had been used to study the role of intermediate signalling events including Gq_{11} and Ca^{2+} – dependent pathways (Macfarlane *et al.*, 2005). We found that while SLIGKV-OH, given alone, caused a 20-fold increase in reporter activity luciferase measured at the 4 h time point, both K-12940 and K-14585 caused a concentration-dependent inhibition of luciferase activity over the low micromolar range which compared well with their effects upon radioligand binding (Figure 4 and Table 3). Maximal inhibition was as much as 80%. Trypsin-stimulated luciferase was also significantly inhibited but less effectively, maximal inhibition was approximately 25% at 10 μM concentration of either compound. Neither agent inhibited luciferase activity stimulated by PMA (% inhibition; K-12940 5.0 ± 2.9, K-14585 = 1.0 ± 1.7 n = 3, non-specific (ns) compared with PMA alone), confirming the receptor specificity of the inhibition.

We then examined the effect of K-12940 and K-14585 upon IL-8 production, known to be regulated at least in part by NFκB activation (Yoshida *et al.*, 2007). Alone, SLIGKV-OH stimulated a 40-fold increase in IL-8 production measured at the 24 h time point (Figure 5). Pre-incubation with both compounds causes a substantial and significant inhibition,

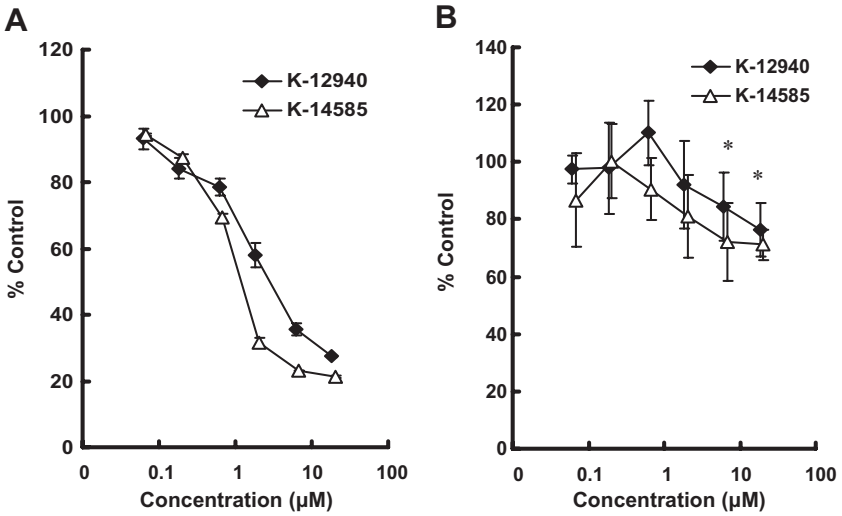

Figure 4 Concentration-dependent inhibitory effects of K-12940 and K-14585 on SLIGKV- or trypsin-mediated NFκB-luciferase activation in NCTC2544 cells. Cells were stimulated with SLIGKV (30 μM) (Panel A) or trypsin (10 nM) (Panel B) in the presence of increasing concentrations of either K-12940 or K-14585. NFκB reporter activity was assayed as outlined in the Methods section. Data represent % of the control activity stimulated with agonist alone ($n = 6$). *$P < 0.05$, compared with control stimulation either peptide or trypsin alone.

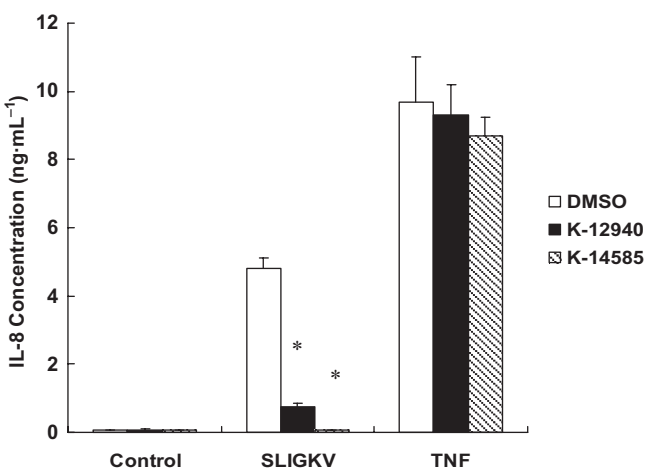

Figure 5 Effect of K-12940 and K-14585 on IL-8 production in NCTC2544-PAR_2 cells. NCTC2544-PAR_2 cells were stimulated with vehicle (Control), SLIGKV (100 μM) or tumuor necrosis factorα (TNFα) (10 ng·mL^{-1}) in the absence (DMSO) or presence of antagonists (5 μM) for 24 h. IL-8 levels in the culture medium were determined by ELISA. Data is expressed as the mean ± SEM of three experiments. *$P < 0.05$ compared with SLIGKV stimulated control.

Table 4 Inhibitory effects of K-14585 on PAR-mediated [^{3}H]-inositol phosphate accumulation in HEK293 cells

HEK293	*Agonist*	*Fold stimulation*			
		Control		*K-14585 (10 μM)*	
		Mean	*SEM*	*Mean*	*SEM*
PAR_1	TFLLR-NH_2	4.76	1.23	5.30	1.61
PAR_2	SLIGKV-OH	5.34	1.60	2.39*	0.48
PAR_4	AYPGKF-NH_2	4.97	0.57	5.57	0.81

*$P < 0.05$ compared with SLIGKV-OH.
$n = 4$.
HEK293 cells were transiently transfected with wild type PAR_1, PAR_2 or PAR_4 plasmid DNA then treated with 10 μM of compound K-14585 followed by stimulation with 30 μM of PAR-specific agonist peptides, TFLLR-NH_2 for PAR_1, SLIGKV-OH for PAR_2, and 100 μM AYPGKF-NH_2 for PAR_4 expressing cells. Total inositol phosphate accumulation was assessed as outlined in the Methods section.
HEK293, human embryonic kidney 293 cells; PAR, proteinase-activated receptor; SLIGKV-OH, Ser-Leu-Ile-Gly-Lys-Val.

K-14585 reducing IL-8 production by over 90%. In contrast, both compounds had no significant effect upon Il-8 production stimulated by TNFα.

Having established the potential for PAR_2 antagonists to affect a series of parameters at the cellular level, we sought to investigate possible effects of K-14585, the more potent of the two compounds on *in vitro* and *in vivo* vascular responses. However, because tissue systems often contain other PARs such as PAR_1 and PAR_4, we first of all tested whether K-14585 was able to cross-react with either of these receptors. Human PARs 1, 2 and 4 were transfected into HEK293 cells and stimulated with the relevant PAR activating peptides (Table 4). While K-14585 (10 μM) caused a significant decrease in PAR_2 peptide-induced [^{3}H]IP accumulation, the compound displayed no equivalent inhibitory effect upon PAR_1- or PAR_4-mediated responses, suggesting selectivity of action.

Having established a lack of cross reactivity of K-14585 on PAR_1 and PAR_4, we examined the endothelium-dependent relaxation of isolated aorta, a well-recognized effect of PAR_2 activation (Figure 6). The rodent-specific activating peptide SLIGRL-NH_2 caused a concentration-dependent decrease in contractile tone, with an EC_{50} value of 1.2 μM. However, in the presence of 10 μM, K-14585, this curve was shifted to the right in a parallel fashion giving an EC_{50} value of 3.2 μM which was significantly different from the control value ($P < 0.001$ Bonferroni's test, Figure 6B). Although this displacement was small and precluded an accurate estimation of K_d, an approximate value of 3.86 μM, derived from the Gaddum equation, was close to the K_i values obtained in the ligand binding experiments and was in the same range of effect

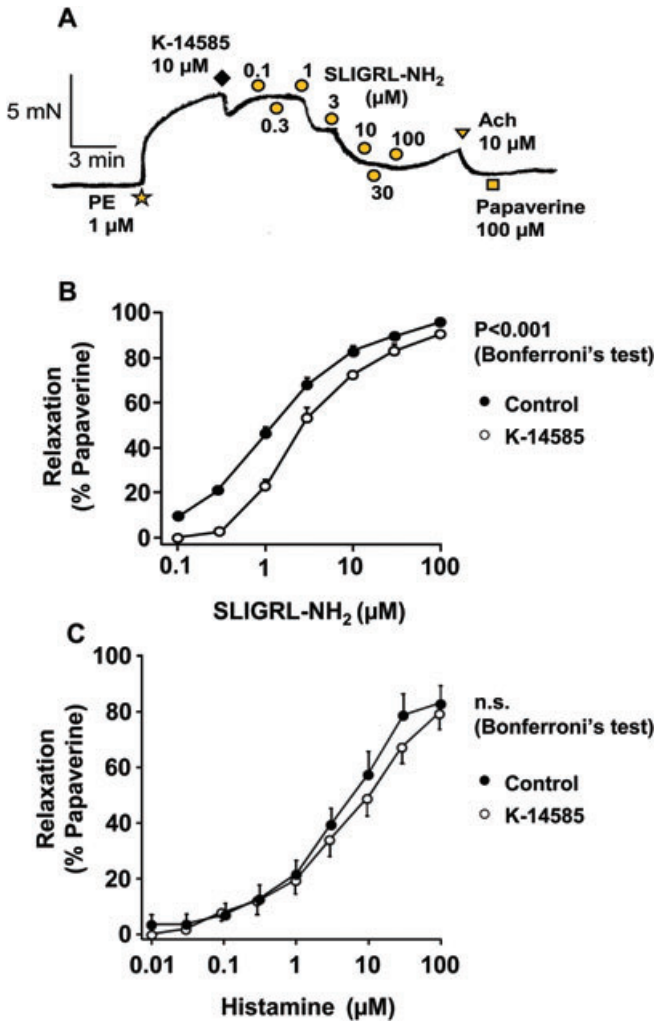

Figure 6 Effect of K-14585 on relaxation of rat aortic rings induced by the proteinase-activated receptor 2 (PAR_2) agonist, Ser-Leu-Ile-Gly-Arg-Leu-amide (SLIGRL-NH_2). In A, SLIGRL-NH_2 was applied cumulatively to the aortic ring preparation pre-contracted with 1 μM phenylephrine (PE). K-14585 (10 μM) was added to the bath 2 min prior to the addition of SLIGRL-NH_2. Summary data (in B) are the mean ± SEM of nine control experiments and 16 with K-14585. The response curve was significantly shifted to the right by K-14585; $P < 0.001$ compared with the control curve (Bonferoni's test). In C, results from experiments using histamine instead of PAR_2 activating peptide and data shown are the mean ± SEM of eight experiments. n.s., not significant.

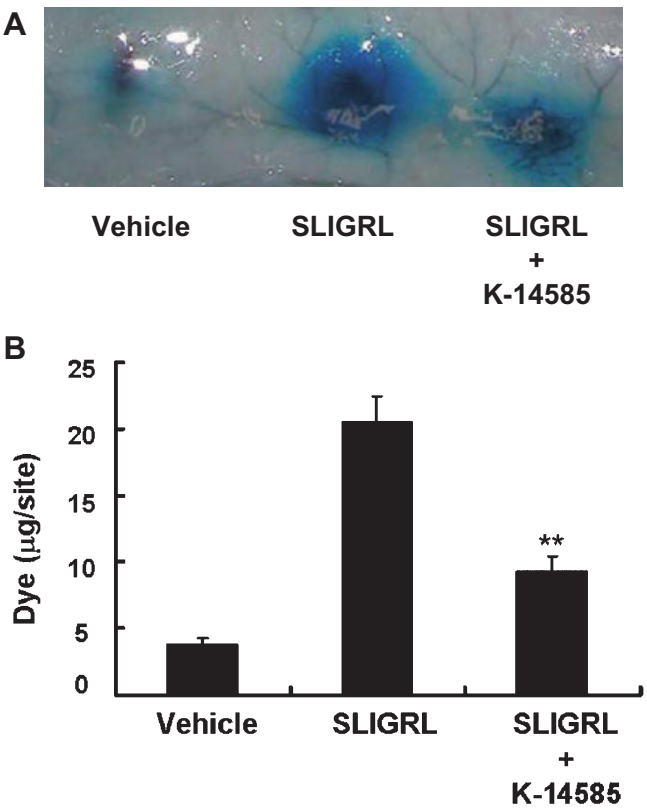

Figure 7 Effect of K-14585 on the plasma exudation caused by the proteinase-activated receptor 2 agonist, Ser-Leu-Ile-Gly-Arg-Leu-amide (SLIGRL-NH_2), in guinea pig dorsal skin. Evans blue dye (50 mg·kg^{-1}) was injected intravenously in male Hartley guinea pigs. Immediately after the dye injection, vehicle (10% DMSO), SLIGRL-NH_2 (300 nM) or a mixture of SLIGRL-NH_2 (300 n^M) and K-14585 (300 μg) was injected intradermally on dorsal skin in a volume of 100 μL per site. Dye extravasation (in A) was quantified (in B) spectrophotometrically, as outlined in the Methods section. Each value represents the mean ± SEM from at least four experiments. *$P < 0.01$ compared with test control (SLIGRL-NH_2).

observed in the cellular assays. In contrast, relaxant responses to histamine were not modified by K-14585, EC_{50} values for histamine alone, 3.1 μM, and in the presence of K-14858, 4.2 μM, were not significantly different (Figure 6C).

We then examined the effect of K-14585 on two variables *in vivo*, vascular permeability assessed by exudation of Evans blue dye (Figure 7) and secretion of saliva (Figure 8). The agonist peptide, SLIGRL-NH_2, caused a substantial increase in dye exudation, assessed in four different animals (Figure 7A) and this effect was significantly reduced by pre-treatment with K-14585 ($P < 0.05$). A similar effect was observed when saliva secretion was examined. Two doses of the PAR_2 activating peptide were used, 1.5 and 2.5 mmol·kg^{-1}. Both stimulated a marked increase in saliva reaching a peak within 10 min before decreasing again at 15 min (Figure 8A). Pre-treatment with K-14585 reduced saliva secretion in response to the lower dose of agonist at 15 min, but the responses to the higher dose were not significantly affected. Similarly, when the response to the lower dose of SLIGRL-NH_2 was expressed as the total saliva collected over 15 min, this total was significantly reduced by K-14585, whereas saliva secretion in response to the higher dose of agonist was unaffected (Figure 8B)

Discussion

In this study, we examined the effects of novel PAR_2 antagonist peptides in a series of assays both *in vitro* and *in vivo*. Initially, we examined a series of compounds on PAR_2 -induced intracellular Ca^{2+} mobilization and identified K-12490 and K-14585 as moderately effective inhibitors. PAR_2 has been shown to mediate Ca^{2+} mobilization in a large number of cell types, including keratinocytes (Santulli *et al.*, 1995), neurons (Bushell *et al.*, 2006) and endothelial cells. In these cell types, Ca^{2+} mobilization is predominantly *Pertussis* toxin-independent (Bushell *et al.*, 2006) and involves Gq_{11} in

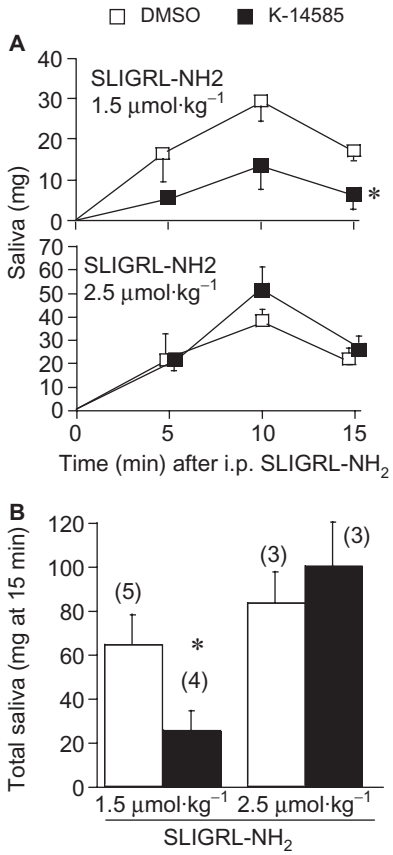

Figure 8 The effect of K-14585 on saliva secretion in anaesthetized mice. K-14585 at 10 μmol·kg^{-1} dissolved in DMSO was administered i.p. in a volume of 10 μL per 10 g body weight, 5 min before i.p. Ser-Leu-Ile-Gly-Arg-Leu-amide (SLIGRL-NH_2) at 1.5 or 2.5 μM, in combination with amastatin at 2.5 μM. Saliva secretion was measured at 5 min intervals for 15 min [basal levels at time 0 were below detection (1 mg)]. Control animals received only the same volume of vehicle (DMSO) before the agonist peptide. Summary results from the whole 15 min collection period are shown in histogram form (in B) and each value represents the mean ± SEM. *$P < 0.001$ compared with control; numbers of animals are shown in parentheses.

the coupling to $InsP_3$ production and subsequent intracellular Ca^{2+} release, although this has not been investigated directly. Recently, we have shown that the novel Gq_{11} inhibitor YM254890 is able to inhibit InsP production (Goon Goh *et al.*, 2008) and intracellular Ca^{2+} mobilization in NCTC2544-PAR_2 cells (Bushell and Plevin, unpublished), results consistent with this model. In other experiments, we also demonstrated that both K-12490 and K-14585 inhibited [^{3}H]InsP in the same cell line, suggesting inhibition of a Gq_{11} coupled PAR_2 response.

Nevertheless, in order to establish that these compounds were directly interacting with the receptor, we examined the compounds in a peptide ligand binding assay utilizing a clonal cell line exogenously expressing PAR_2 (Kanke *et al.*, 2001). This cell line was initially found to express no endogenous PAR_2, no PAR_3 or PAR_4 and a minor amount of PAR_1 (Kawabata *et al.*, 2004; Kanke *et al.*, 2005). Competition curves indicated that these compounds competed with [^{3}H]2-furoyl-LIGRL-NH_2 binding to the receptor with affinities close to their inhibitory potency at the level of Ca^{2+} mobilization. Slopes close to unity suggested that K-12940 and K-14585 are competitive PAR_2 antagonists, however, this needs to be examined in more detail. As there is no binding of radiolabelled peptide in cells which do not express the receptor (Kanke *et al.*, 2005), this suggests competitive binding to PAR_2; however, it is possible, although unlikely, that displacement of radiolabelled 2-furoyl-LIGRL-NH_2 is artifactual and that the K compounds bind directly to the radioligand.

We next assessed the potential of K-14585 to inhibit a number of selected cellular events relevant to the biological actions of PAR_2. Activation of this receptor has been shown by ourselves and others to link strongly to the NFκB pathway primarily via Gq_{11} and Ca^{2+}-dependent mediated events (Kanke *et al.*, 2001; Macfarlane *et al.*, 2005; Goon Goh *et al.*, 2008) which in turn is involved in regulation of IL-8 production (Yoshida *et al.*, 2007). Although both compounds were active against agonist peptide stimulation of NFκB and IL-8 production, we consistently found that trypsin-stimulated responses, including that of NFκB were inhibited to a much lesser extent. The reasons for this are unclear and given the K_i values of K-14585 for binding to PAR_2 (0.627 μM) and the maximum concentration used in several assays of 10 μM, one might theoretically expect greater inhibition. It is therefore possible that K-14585 competes more effectively for peptide binding to a site which is distinct from, or at least only partially overlapping, that occupied by the tethered ligand. This possibility has been raised although not conclusively proved for PAR_1 activating peptides (Blackhart *et al.*, 2000). In addition, the data tentatively suggest the potential for agonist-directed signalling; peptide and tethered ligand activate a different pattern of signalling pathways such that inhibition of downstream parameters such as NFκB activity by the K compounds reflects inhibition of only the signalling pathways that the peptide can induce and not the tethered ligand. This possibility is currently being examined in our laboratory.

This difference in affinity between the activating serine protease and cognate activating peptide has been observed before, for the other PARs (Macfarlane *et al.*, 2001). Recently, however, one group successfully developed a competitive PAR_1 antagonist, RWJ-56110, which can effectively inhibit both agonist peptide-activated and proteolytically activated receptor (Andrade-Gordon *et al.*, 1999; Maryanoff *et al.*, 2003), suggesting a common site of receptor interaction for the PAR_1 peptide and tethered ligand in these examples. Therefore, the PAR_2 antagonists identified in this study still may represent appropriate leads for the future development of high affinity antagonists.

A limitation of our current investigation is the structure of the compounds studied. There was a need for a peptide structure and a precise requirement for bulky moieties at the C-terminus, which made the compounds more complicated in structure and less soluble in water. This limited the use of these compounds at higher concentrations because of problems of solubility. Nevertheless, the SAR analysis of these compounds highlighted some strict structural requirement for PAR_2 antagonism. Firstly, the importance of the N-terminal N-heteroaromatic urea portion; secondly, the basic functionality on the amino side chain; and thirdly, the C-terminal hydrophobic group. For example the indol-5-yl isomer of

K-14585 lost all antagonist activity (not shown). Furthermore, there may be additional structural requirements to aid resistance to degradation in tissues; this aspect has not been examined in this study but was a feature of the substituted agonist peptide, 2-furoyl-LIGRL-OH (Kawabata *et al*., 2004).

Despite the limitations of the antagonists described in this study in terms of potency, any potential actions *in vitro* and *in vivo* would be an important aspect of antagonist actions. Endothelium-dependent relaxations of blood vessels is an established feature of the actions of PAR_2 mediated by a predominantly nitric oxide (NO)-dependent mechanism (AlAni *et al*., 1995; Hwa *et al*., 1996; Sobey and Cocks, 1998). The most potent compound, K-14585, caused a parallel shift in the concentration indicative of competitive antagonism with the estimated K_d value in the low micromolar range consistent with that obtained in other assays. However, the actions of PAR_2–mediated effects upon endothelial function are not limited to vasodilatation and we recorded similar inhibitory effects of K-14585 upon vascular permeability. For both these parameters, inhibition was not always complete and sometimes less effective at higher concentrations, suggestive of solubility problems (Figures 6 and 8). Nevertheless, PAR_2 has been shown to directly regulate endothelial barrier function as a component of a cellular response which includes leucocyte rolling, adhesion and extravasation in endothelial cells (Vergnolle *et al*., 1999a) and the inhibition described here is consistent with blocking this action. These effects are manifested *in vivo*, as intraplantar injection of PAR activating peptide induced significant oedema in the rat hind paw which was followed by a disruption of tissue architecture along with an inflammatory cell infiltrate (Vergnolle *et al*., 1999b) and PAR_2 deficient mice show a delayed onset of leucocyte rolling and adhesion following inflammatory challenge (Lindner *et al*., 2000). These actions may be via a direct effect on the prostanoids (Kong *et al*., 1997) and NO (Hwa *et al*., 1996), although a neurogenic mechanism may also be involved, in turn, via the release of calcitonin gene-related peptide and substance P (Steinhoff *et al*., 2000). Similar mechanisms of regulation are also observed for PAR_2 regulation of salivary gland function (Kawabata *et al*., 1999; 2000; 2002), the inhibition of this process by K-14585 suggests a common receptor existing in different tissues, susceptible to competitive antagonism.

In conclusion, this study identifies a moderately potent competitive PAR_2 antagonist, K-14585 which was effective against PAR_2 activating peptides in cellular assays and *in vitro* systems and may be utilized to further characterize the effects mediated by PAR_2. However, at present, its usefulness in probing PAR_2 functions mediated by protease activators of PARs is limited. Nevertheless, while further studies are required to develop potent bio-available, non-peptide, antagonists, the compound described in this study provides an attractive template for such future studies.

Acknowledgements

This work was supported by Kowa Company Ltd., Japan. Margaret R Cunningham is a recipient of an AJ Clark studentship award from The British Pharmacological Society.

Statement of conflict of interest

None.

References

AlAni B, Saifeddine M, Hollenberg MD (1995). Detection of functional receptors for the proteinase-activated-receptor-2-activating polypeptide, SLIGRL-NH2, in rat vascular and gastric smooth muscle. *Can J Physiol Pharmacol* **73**: 1203–1207.

Alexander SP, Mathie A, Peters JA (2008). Guide to receptors and channels (GRAC), 3rd edition. *Br J Pharmacol* **153** (Suppl. 2): S1–S209.

Andrade-Gordon P, Maryanoff BE, Derian CK, Zhang HC, Addo MF, Darrow AL *et al*. (1999). Design, synthesis, and biological characterization of a peptide-mimetic antagonist for a tethered-ligand receptor. *Proc Natl Acad Sci USA* **96**: 12257–12262.

Blackhart BD, Ruslim-Litrus L, Lu CC, Alves VL, Teng W, Scarborough RM *et al*. (2000). Extracellular mutations of protease-activated receptor-1 result in differential activation by thrombin and thrombin receptor agonist peptide. *Mol Pharmacol* **58**: 1178–1187.

Bushell TJ, Plevin R, Cobb S, Irving AJ (2006). Characterization of proteinase-activated receptor 2 signalling and expression in rat hippocampal neurons and astrocytes. *Neuropharmacology* **50**: 714–725.

Camerer E, Gjernes E, Wiiger M, Pringle S, Prydz H (2000). Binding of Factor VIIa to tissue factor on keratinocytes induces gene expression. *J Biol Chem* **275**: 6580–6585.

Cenac N, Coelho AM, Nguyen C, Compton S, Andrade-Gordon P, MacNaughton WK *et al*. (2002). Induction of intestinal inflammation in mouse by activation of proteinase-activated receptor-2. *Am J Pathol* **161**: 1903–1915.

Cocks TM, Moffatt JD (2000). Protease-activated receptors: sentries for inflammation? *Trends Pharmacol Sci* **21**: 103–108.

Ferrell WR, Lockhart JC, Kelso EB, Dunning L, Plevin R, Meek SE *et al*. (2003). Essential role for proteinase-activated receptor-2 in arthritis. *J Clin Invest* **111**: 35–41.

Goon Goh F, Sloss CM, Cunningham MR, Nilsson M, Cadalbert L, Plevin R (2008). G-protein-dependent and -independent pathways regulate proteinase-activated receptor-2 mediated p65 NFkappaB serine 536 phosphorylation in human keratinocytes. *Cell Signal* **20**: 1267–1274.

Hollenberg MD (2005). Physiology and pathophysiology of proteinase-activated receptors (PARs): proteinases as hormone-like signal messengers: PARs and more. *J Pharmacol Sci* **97**: 8–13.

Hwa JJ, Ghibaudi L, Williams P, Chintala M, Zhang RM, Chatterjee M *et al*. (1996). Evidence for the presence of a proteinase-activated receptor distinct from the thrombin receptor in vascular endothelial cells. *Circ Res* **78**: 581–588.

Kaneider NC, Leger AJ, Agarwal A, Nguyen N, Perides G, Derian C *et al*. (2007). 'Role reversal' for the receptor PAR1 in sepsis-induced vascular damage. *Nat Immunol* **8**: 1303–1312.

Kanke T, Macfarlane SR, Seatter MJ, Davenport E, Paul A, McKenzie RC *et al*. (2001). Proteinase-activated receptor-2-mediated activation of stress-activated protein kinases and inhibitory kappa B kinases in NCTC 2544 keratinocytes. *J Biol Chem* **276**: 31657–31666.

Kanke T, Ishiwata H, Kabeya M, Saka M, Doi T, Hattori Y, Kawabata A, Plevin R (2005). Binding of a highly potent protease-activated receptor-2 (PAR2) activating peptide, [3H]2-furoyl-LIGRL-NH2, to human PAR2. *Br J Pharmacol* **145**: 255–263.

Kawabata A, Hollenberg MD, Kuroda R (1998). Effects of trypsin and a selective agonist peptide of proteinase-activated receptor 2 on vascular permeability in rat hindpaw. *Naunyn Schmiedebergs Arch Pharmacol* **358**: 3797.

Kawabata A, Kuroda R, Nishikawa H, Kawai K (1999). Modulation by protease-activated receptors of the rat duodenal motility in vitro:

possible mechanisms underlying the evoked contraction and relaxation. *Br J Pharmacol* **128**: 865–872.

Kawabata A, Morimoto N, Nishikawa H, Kuroda R, Oda Y, Kakehi K (2000). Activation of protease-activated receptor-2 (PAR-2) triggers mucin secretion in the rat sublingual gland. *Biochem Biophys Res Commun* **270**: 298–302.

Kawabata A, Kinoshita M, Nishikawa H, Kuroda R, Nishida M, Araki H *et al*. (2001). The protease-activated receptor-2 agonist induces gastric mucus secretion and mucosal cytoprotection. *J Clin Invest* **107**: 1443–1450.

Kawabata A, Kuroda R, Nishida M, Nagata N, Sakaguchi Y, Kawao N *et al*. (2002). Protease-activated receptor-2 (PAR-2) in the pancreas and parotid gland: immunolocalization and involvement of nitric oxide in the evoked amylase secretion. *Life Sci* **71**: 2435–2446.

Kawabata A, Kanke T, Yonezawa D, Ishiki T, Saka M, Kabeya M *et al*. (2004). Potent and metabolically stable agonists for protease-activated receptor-2: evaluation of activity in multiple assay systems in vitro and in vivo. *J Pharmacol Exp Ther* **309**: 1098–1107.

Kawagoe J, Takizawa T, Matsumoto J, Tamiya M, Meek SE, Smith AJ *et al*. (2002). Effect of protease-activated receptor-2 deficiency on allergic dermatitis in the mouse ear. *Jpn J Pharmacol* **88**: 77–84.

Kawao N, Sakaguchi Y, Tagome A, Kuroda R, Nishida S, Irimajiri K *et al*. (2002). Protease-activated receptor-2 (PAR-2) in the rat gastric mucosa: immunolocalization and facilitation of pepsin/pepsinogen secretion. *Br J Pharmacol* **135**: 1292–1296.

Kelso EB, Lockhart JC, Hembrough T, Dunning L, Plevin R, Hollenberg MD *et al*. (2006). Therapeutic promise of proteinase-activated receptor-2 antagonism in joint inflammation. *J Pharmacol Exp Ther* **316**: 1017–1024.

Kong W, McConalogue K, Khitin LM, Hollenberg MD, Payan DG, Bohm SK *et al*. (1997). Luminal trypsin may regulate enterocytes through proteinase-activated receptor 2. *Proc Natl Acad Sci (USA)* **94**: 8884–8889.

Lan RS, Stewart GA, Henry PJ (2000). Modulation of airway smooth muscle tone by protease activated receptor-1,-2,-3 and-4 in trachea isolated from influenza A virus-infected mice. *Br J Pharmacol* **129**: 63–70.

Lan RS, Knight DA, Stewart GA, Henry PJ (2001). Role of PGE(2) in protease-activated receptor-1, -2 and -4 mediated relaxation in the mouse isolated trachea. *Br J Pharmacol* **132**: 93–100.

Lindner JR, Kahn ML, Coughlin SR, Sambrano GR, Schauble E, Bernstein D *et al*. (2000). Delayed onset of inflammation in protease-activated receptor-2- deficient mice. *J Immunol* **165**: 6504–6510.

Macfarlane SR, Seatter MJ, Kanke T, Hunter GD, Plevin R (2001). Proteinase-activated receptors. *Pharmacol Rev* **53**: 245–282.

Macfarlane SR, Sloss CM, Cameron P, Kanke T, McKenzie RC, Plevin R (2005). The role of intracellular Ca2+ in the regulation of proteinase-activated receptor-2 mediated nuclear factor kappa B signalling in keratinocytes. *Br J Pharmacol* **145**: 535–544.

Maryanoff BE, Zhang HC, Andrade-Gordon P, Derian CK (2003). Discovery of potent peptide-mimetic antagonists for the human thrombin receptor, protease-activated receptor-1 (PAR-1). *Curr Med Chem Cardiovasc Hematol Agents* **1**: 13–36.

Molino M, Barnathan ES, Numerof R, Clark J, Dreyer M, Cumashi A *et al*. (1997). Interactions of mast cell tryptase with thrombin receptors and PAR-2. *J Biol Chem* **272**: 4043–4049.

Mototsugu K, Kyoko Y, Toru K, Hioryuki I, Junya T (2007). PAR-2 antagonists EP1806141 (A1); 2007/7/11.

Nystedt S, Emilsson K, Wahlestedt C, Sundelin J (1994). Molecular cloning of a potential proteinase activated receptor [see comments]. *Proc Natl Acad Sci USA* **91**: 9208–9212.

Plevin R, Kellock NA, Wakelam MJ, Wadsworth R (1994). Regulation by hypoxia of endothelin-1-stimulated phospholipase D activity in sheep pulmonary artery cultured smooth muscle cells. *Br J Pharmacol* **112**: 311–315.

Ricciardolo FLM, Steinhoff M, Amadesi S, Guerrini R, Tognetto M, Trevisani M *et al*. (2000). Presence and bronchomotor activity of protease-activated receptor-2 in guinea pig airways. *Am J Respir Crit Care Med* **161**: 1672–1680.

Santulli RJ, Derian CK, Darrow AL, Tomko KA, Eckardt AJ, Seiberg M *et al*. (1995). Evidence for the presence of a protease-activated receptor distinct from the thrombin receptor in human keratinocytes. *Proc Natl Acad Sci U S A* **92**: 9151–9155.

Scott G, Leopardi S, Printup S, Malhi N, Seiberg M, Lapoint R (2004). Proteinase-activated receptor-2 stimulates prostaglandin production in keratinocytes: analysis of prostaglandin receptors on human melanocytes and effects of PGE2 and PGF2alpha on melanocyte dendricity. *J Invest Dermatol* **122**: 1214–1224.

Sobey CG, Cocks TM (1998). Activation of protease-activated receptor-2 (PAR-2) elicits nitric oxide-dependent dilatation of the basilar artery in vivo. *Stroke* **29**: 1439–1444.

Steinhoff M, Vergnolle N, Young SH, Tognetto M, Amadesi S, Ennes HS *et al*. (2000). Agonists of proteinase-activated receptor 2 induce inflammation by a neurogenic mechanism. *Nat Med* **6**: 151–158.

Steinhoff M, Buddenkotte J, Shpacovitch V, Rattenholl A, Moormann C, Vergnolle N *et al*. (2005). Proteinase-activated receptors: transducers of proteinase-mediated signaling in inflammation and immune response. *Endocr Rev* **26**: 1–43.

Takeda Y, Krause JE (1989). Neuropeptide K potently stimulates salivery gland secretion and potentiates substance P-induced salivation. *PNAS* **86**: 392–396.

Vergnolle N, McKnight W, Befus AD, Hollenberg MD, Wallace JL (1998). Induction of an inflammatory response by activation of protease-activated receptor 2 (PAR-2). *Naunyn Schmiedebergs Arch Pharmacol* **358**: 573.

Vergnolle N, Hollenberg D, Wallace JL, Morley MD (1999a). Activation of proteinase-activated receptor-2 (PAR-2) induces leukocyte adhesion. *FASEB J* **13**: A668.

Vergnolle N, Hollenberg MD, Sharkey KA, Wallace JL (1999b). Characterization of the inflammatory response to proteinase-activated receptor-2 (PAR(2))-activating peptides in the rat paw. *Br J Pharmacol* **127**: 1083–1090.

Yoshida N, Katada K, Handa O, Takagi T, Kokura S, Naito Y *et al*. (2007). Interleukin-8 production via protease-activated receptor 2 in human esophageal epithelial cells. *Int J Mol Med* **19**: 335–340.